Split-Spectrum InSAR for Reliable Ionospheric Correction: A Critical Review of Uncertainty, Validation, and Reproducibility

Mohit Sheode

Department of Civil Engineering, Maulana Azad National Institute of Technology, Bhopal, Madhya Pradesh, India

Correspondence: mhtsht@gmail.com

ORCID: https://orcid.org/0009-0009-5719-5084

Article type	Critical narrative review
Preprint version	Version 1 - 5 August 2026
Peer-review status	Not peer reviewed; not currently under journal consideration
Supporting record	Synthetic arrays, parameter settings, numerical outputs, and figure-generating code are available from the corresponding author upon reasonable request.

Journal-status statement: *An earlier version of this manuscript was submitted for publication in the SSRG International Journal of Geo-informatics and Geological Science but is no longer under consideration by that journal. The manuscript has not been formally accepted for publication. Subsequent versions may contain revisions arising from community feedback or submission to another journal. Please feel free to contact the author; feedback is welcome.*

Critical Narrative Review

Split-Spectrum InSAR for Reliable Ionospheric Correction: A Critical Review of Uncertainty, Validation, and Reproducibility

Mohit Sheode

Department of Civil Engineering, Maulana Azad National Institute of Technology, Bhopal, Madhya Pradesh, India.

Corresponding author: mhtsht@gmail.com | ORCID: https://orcid.org/0009-0009-5719-5084

Abstract. Split-spectrum interferometry provides a physically grounded means of separating dispersive ionospheric phase from non-dispersive deformation-related phase in Interferometric Synthetic Aperture Radar observations. Its practical reliability, however, depends on processing choices that are often reported incompletely and validated inconsistently. This critical narrative review examines the physical basis of range split-spectrum correction and synthesizes representative literature on sub-band design, sensor and acquisition-mode dependence, coherence loss, filtering, phase unwrapping, parameter errors, and time-series application. A structured reporting audit of 25 scholarly sources shows that sensor context is usually documented, whereas spectral design, reproducibility, and uncertainty are frequently only partially reported. The review identifies a central trade-off between increased sensitivity to frequency-dependent phase and reduced stability as usable sub-band bandwidth narrows. To make reliability quantitatively operational, it states the standard phase-separation coefficients, provides covariance-aware uncertainty propagation, and translates the method into a reproducible processing sequence. It proposes that an operational correction should be accompanied by three linked products: the estimated ionospheric phase, the corrected interferometric phase, and a spatially explicit uncertainty or reliability layer. A minimum reporting framework is developed for sensor context, spectral design, interferometric processing, ionospheric estimation, validation, reproducibility, and uncertainty. Cross-sensor benchmark datasets representing different radar bands, environments, coherence regimes, and acquisition modes are recommended. The resulting framework shifts evaluation from visual phase improvement toward transparent, quantitative, and reproducible evidence that the corrected deformation signal can be trusted.

Keywords: InSAR, ionospheric correction, reproducibility, split-spectrum interferometry, uncertainty quantification

1. Introduction

Interferometric Synthetic Aperture Radar (InSAR) has transformed the observation of earthquakes, volcanic unrest, land subsidence, glacier motion, and slope instability by measuring surface displacement over large areas with high phase sensitivity. [1-4,10-13,21]

An interferogram, however, does not contain deformation alone. Orbital inaccuracies, topographic residuals, temporal decorrelation, tropospheric delay, and ionospheric disturbances can all contribute to the measured phase. Without adequate separation, an atmospheric or instrumental artefact may be interpreted as genuine ground movement.

Ionospheric contamination is especially important for long-wavelength radar systems. Variations in free-electron density can introduce broad phase gradients, streaks, azimuth shifts, and spatially variable distortions. These effects are often strongest in L-band observations, although C-band interferograms can also be affected during disturbed ionospheric conditions or when subtle long-wavelength deformation is analyzed. [2-4,8,10-13,19,21,24]

Split-spectrum interferometry offers a physically grounded response. The available radar bandwidth is divided into separate frequency sub-bands and the resulting interferograms are compared. Because non-dispersive and ionospheric phase components scale differently with radar frequency, their contributions can be estimated separately. [1,2,7,9,14,16,17,25]

The principle is elegant, but the result is not automatically reliable. Sub-band design, coherence, filtering, unwrapping, sensor characteristics, parameter accuracy, and validation choices influence the correction. This review argues that the next major advance should be a common framework for reporting, validating, and comparing split-spectrum results across sensors, acquisition modes, and environments.

2. Review Scope and Analytical Framework

This article is a critical narrative review rather than a systematic or exhaustive evidence synthesis. The scholarly literature was assembled through iterative, targeted searches of publication titles and keyword fields using combinations of "InSAR," "ionospheric correction," "split spectrum," "range split spectrum," "azimuth split spectrum," "total electron content," "uncertainty," and "validation." Candidate publications were supplemented through backward reference chaining from foundational method papers and major review articles. The search was designed to identify a representative body of literature relevant to the review questions rather than to establish complete database coverage.

Each candidate source was screened for direct relevance to at least one of six analytical themes: physical phase separation, processing trade-offs, sensor or acquisition-mode dependence, validation, uncertainty communication, and reproducibility. Duplicate, tangential, and general InSAR studies without a material connection to ionospheric estimation or spectral-diversity processing were excluded. The final analytical corpus comprised 25 scholarly publications [1-25]. Official processing and mission documentation were consulted separately and were not counted within the scholarly corpus [26-28]. The synthesis is therefore focused and interpretive and does not use meta-analytic weighting.

The publications are interpreted through the six linked themes above to identify the minimum evidence required before an ionospheric correction is treated as a dependable deformation product. To make the central reporting-gap claim auditable, the 25 scholarly sources were also coded against the seven reporting elements later defined in Table 2: sensor context, spectral design, interferometric processing, ionospheric estimation, validation, reproducibility, and uncertainty.

3. Physical Basis and Methodological Scope

3.1. Separating Dispersive and Non-Dispersive Phase

A conventional interferogram contains several phase components. Surface displacement, topographic residuals, and most propagation effects behave as non-dispersive contributions, whereas ionospheric phase is dispersive and varies inversely with radar frequency. [1,6,9-14,21,24]

In range split-spectrum processing, the range spectrum is separated into lower-frequency and higher-frequency sub-bands. An interferogram is generated from each sub-band. Both observe the same underlying ground deformation but contain different ionospheric phase contributions. A frequency-dependent linear combination can therefore isolate the dispersive component and recover the non-dispersive phase more reliably. [1,2,7,14,16,17,25]

Let φ_H and φ_L denote the unwrapped interferometric phases of the high- and low-frequency sub-bands, whose center frequencies are f_H and f_L, and let f0 be the center frequency of the original full-band observation. The ionospheric phase referenced to f0 can be expressed as follows. [1,14,17,25]

$$\varphi_{\text{iono}} = a\varphi_{\text{H}} + b\varphi_{\text{L}} \qquad (1)$$

$$a = \frac{f_L f_H^2}{f_0(f_H^2 - f_L^2)} \quad (2)$$

$$b = \frac{-f_L^2 f_H}{f_0(f_H^2 - f_L^2)} \quad (3)$$

The corrected full-band phase is obtained by subtracting the ionospheric estimate in Equation (1) from the full-band interferometric phase. Because the magnitudes of a and b increase when the effective sub-band separation becomes small relative to the carrier frequency, sub-band phase noise is amplified in the ionospheric estimate. This mathematical amplification is the basis of the sensitivity–stability trade-off discussed below.

The procedure depends on a coupled set of spectral-design, interferometric-processing, and quality-control choices:

- sub-band bandwidth and center-frequency separation;
- spectral overlap or guard-band configuration;
- common-band filtering and coregistration accuracy;
- coherence thresholds and masking rules;
- phase filtering and unwrapping strategy;
- smoothing scale applied to the ionospheric estimate; and
- treatment of low-coherence, missing, or discontinuous pixels.

These are not minor implementation details. They control sensitivity, phase noise, spatial resolution, and the stability of the estimated ionospheric screen. Their effects become especially important when bandwidth or coherence is limited. [1,5,16,17,22,25]. A smoother interferogram is not, by itself, proof of a more accurate deformation measurement.

3.2. Split Spectrum is Not One Universal Workflow

The term split spectrum covers related but distinct uses of spectral diversity. Range split-spectrum processing is commonly used to estimate dispersive ionospheric phase. Azimuth split-spectrum or multiple-aperture methods use Doppler-domain separation to estimate ionosphere-induced azimuth shifts. Split-bandwidth approaches may also extend the measurable displacement range where deformation gradients are too large for conventional interferometry. [2,6,9,12,14,15,18,20,25]

These methods share a broad spectral-diversity principle but do not estimate the same quantity and should not be evaluated under identical assumptions. Even within range split-spectrum correction, a workflow designed for one mission cannot be transferred automatically to another. L-band and C-band sensors differ in wavelength, usable bandwidth, ionospheric sensitivity, and typical coherence behavior, while Stripmap, TOPS, and ScanSAR modes introduce additional processing constraints. [2-4,8,9,19,21,23-25]

3.3. Operational Processing Workflow

A reproducible range split-spectrum implementation can be organized into eight stages: (1) ingest complex Single Look Complex data and define the common acquisition support; (2) generate low- and high-frequency sub-bands by range-frequency band-pass filtering; (3) co-register the full-, low-, and high-band pairs using consistent geometry and estimated shifts; (4) form the three interferograms and estimate coherence; (5) apply documented multilooking and phase filtering; (6) unwrap the required full- and sub-band phase combinations; (7) estimate, screen, and spatially filter the ionospheric phase; and (8) subtract the accepted ionospheric estimate from the full-band phase, validate the result, and publish the associated reliability layer. [1,2,17,23,25]

In ESA SNAP 13, a TOPS implementation uses Bandpass Filter immediately after TOPSAR-Split to produce the low and high sub-bands. The overall range and azimuth shifts estimated through Enhanced Spectral Diversity for the full-band pair should be reused for the sub-band pairs. Interferogram formation with coherence estimation is followed by debursting, Goldstein phase filtering, multilooking, SNAPHU unwrapping, and the Ionospheric Correction operator. Stripmap data follow the same principle, with band-pass filtering applied directly after SLC ingestion. This sequence is one documented implementation rather than a universal software requirement. [1,26]

4. Processing Trade-offs and Sources of Uncertainty

4.1. Sensitivity Versus Stability

The original Synthetic Aperture Radar bandwidth determines range resolution and the signal information available to the processor. Dividing it into sub-bands reduces the bandwidth assigned to each interferogram. Narrower sub-bands may consequently reduce range resolution and increase phase uncertainty. [1,5,11,16,17,22,25] The principal consequences are summarized in **Table 1**.

Greater separation between the lower and upper center frequencies generally increases sensitivity to the frequency-dependent ionospheric signal. The usable separation is nevertheless limited by the original bandwidth and the need to retain sufficient signal quality in both sub-bands. Frequency separation therefore improves ionospheric sensitivity, while spectral narrowing can amplify noise and reduce measurement stability. This trade-off becomes critical in vegetated, snow-covered, glaciated, or rapidly changing terrain where coherence may already be limited. Recent controlled evaluations further demonstrate a linked trade-off between multilooking and smoothing scale. [1,3,5,8,16,22,25]

Table 1. Principal processing choices and their likely consequences

Processing choice	Likely consequence
Wider frequency separation	Greater sensitivity to dispersive phase, subject to available bandwidth.
Narrower sub-bands	Lower sub-band signal quality and potentially greater phase noise.
Stronger smoothing	More stable large-scale correction, but possible removal of genuine long-wavelength deformation.
Permissive coherence threshold	More spatial coverage, but weaker reliability in noisy areas.
Strict coherence threshold	Higher confidence in retained pixels, but reduced spatial completeness.

4.2. Error Sources and Propagation

Uncertainty can arise from sub-band phase noise, coherence loss, co-registration errors, inaccurate radar parameters, filtering decisions, phase unwrapping, and assumptions made during frequency-dependent phase separation. Parameter and wavenumber errors can propagate into the correction rather than disappearing within the estimator. [5,7,10,16,17,21,22,25]

A reliability description should therefore consider sub-band coherence, phase variance, valid-pixel support, effective frequency separation, and sensitivity to processing parameters. Even a transparent high-, moderate-, or low-confidence classification is more informative than presenting corrected phase as uniformly certain.

5. Validation, Reporting, and Benchmarking

5.1. Validation Must Be Designed into the Workflow

Comparing an interferogram before and after correction is useful but insufficient. A reduced phase ramp does not prove that the removed signal was entirely ionospheric; the correction may also suppress long-wavelength deformation, orbital residuals, or other geophysical signals.

Validation should combine independent evidence and internal consistency tests. Depending on the application, appropriate references include Global Navigation Satellite System displacement, Total Electron Content products, simulated deformation, stable-area statistics, alternative ionospheric corrections, interferometric closure, and temporal consistency across a time series. [3,4,8,15,16,19,20,24,25]

Quantitative metrics should be selected according to the scientific objective and spatial scale of the expected deformation. Suitable measures include:

- root-mean-square error against an independent reference;
- residual phase variance or median absolute deviation;
- reduction in long-wavelength phase power;
- closure residuals across interferometric networks;
- stable-reference-area displacement statistics;
- correlation with Global Navigation Satellite System or Total Electron Content observations; and
- preservation of independently known deformation signals.

For time-series analysis, a correction should improve temporal consistency without suppressing the expected deformation trend. A method that reduces spatial noise but introduces temporal bias is not a successful correction. Comparisons with independent Global Navigation Satellite System observations provide particularly strong evidence when available. [4,7,8,16,19,24]

5.2. The Correction Should Include an Uncertainty Product

Split-spectrum processing is usually presented as a sequence that produces an ionospheric phase screen and a corrected interferogram. A more complete scientific product contains three linked outputs:

1. the estimated ionospheric phase;

2. the corrected interferometric phase; and

3. a spatially explicit uncertainty or reliability layer.

The third output makes clear where the correction is strongly supported, where it depends on interpolation or smoothing, and where low coherence or weak spectral separation prevents confident interpretation.

The reliability layer should be anchored in an explicit error model. Using the coefficients in Equations (2) and (3), first-order propagation gives the following pixel-wise variance when the covariance between sub-band phases is retained.

$$\sigma_{\mathrm{iono}}{}^2 = a^2\sigma_{\mathrm{H}}{}^2 + b^2\sigma_{\mathrm{L}}{}^2 + 2ab\,\mathrm{Cov}(\varphi_{\mathrm{H}}, \varphi_{\mathrm{L}}) \quad (4)$$

If the two sub-band phase errors are assumed independent, the covariance term is omitted:

$$\sigma_{\mathrm{iono}}{}^2 = a^2\sigma_{\mathrm{H}}{}^2 + b^2\sigma_{\mathrm{L}}{}^2 \quad (5)$$

The independence form should not be treated as universally valid because both sub-bands originate from the same acquisitions and may share coregistration, atmospheric, and processing errors. Phase variances may be estimated from sub-band coherence and the effective number of looks, while sensitivity tests should quantify additional uncertainty introduced by masking, unwrapping, interpolation, and smoothing. [1,5,17,22,25]

5.3. Minimum Reporting Standard

Reproducibility does not require every researcher to use the same software or filtering strategy. It requires that relevant decisions are reported clearly enough for another researcher to understand, repeat, and evaluate the workflow. Table 2 provides a compact minimum reporting standard derived from the issues identified in the reviewed literature. [1,5,6,9,17,21-25]

Table 2. Minimum information for reporting split-spectrum ionospheric correction

Reporting element	Minimum information
Sensor context	Mission, radar band, acquisition mode, polarization, orbit geometry, and scene environment.
Spectral design	Original bandwidth, sub-band center frequencies, sub-band bandwidths, frequency separation, overlap, and guard bands.
Interferometric processing	Coregistration method, common-band filtering, coherence threshold, masking, phase filtering, and unwrapping.

Reporting element	Minimum information
Ionospheric estimation	Combination equation or implementation, smoothing scale, interpolation, and treatment of invalid pixels.
Validation	Reference data, stable areas, alternative methods, quantitative metrics, and preservation of deformation signals.
Reproducibility	Software, version, processor or module, key parameters, and any manual intervention.
Uncertainty	Error assumptions, sensitivity tests, residual statistics, and reliability criteria.

To test the reporting-gap claim directly, each of the 25 scholarly publications was coded against the seven elements in Table 2. The publication-level audit is presented in **Table 3**.

Table 3. Reporting coverage across the 25 reviewed scholarly sources

Ref.	SC	SD	IP	IE	V	R	U
[1]	F	F	F	F	F	P	P
[2]	F	F	F	F	F	P	P
[3]	F	P	F	F	F	P	P
[4]	F	P	F	F	F	P	P
[5]	F	P	P	F	F	P	F
[6]	P	P	P	F	P	N	P
[7]	F	F	F	F	F	P	P
[8]	F	P	F	F	F	P	F
[9]	F	F	F	F	P	P	P
[10]	F	N	P	P	P	N	P
[11]	F	N	P	P	P	N	P
[12]	F	N	P	P	P	N	P
[13]	F	N	P	P	P	N	P
[14]	F	P	P	F	P	P	P
[15]	F	F	F	F	F	P	P
[16]	F	F	F	F	F	P	F
[17]	F	F	F	F	P	F	P
[18]	F	F	F	N	F	P	P
[19]	F	N	F	F	F	P	P
[20]	F	F	F	F	F	P	P
[21]	F	P	P	P	N	N	F
[22]	F	F	F	F	F	P	F
[23]	F	F	F	F	P	F	P
[24]	F	P	P	F	P	P	F
[25]	F	F	F	F	F	F	F
F/P/N	**24/1/0**	**12/8/5**	**16/9/0**	**19/5/1**	**14/10/1**	**3/16/6**	**7/18/0**

Note: SC = sensor context; SD = spectral design; IP = interferometric processing; IE = ionospheric estimation; V = validation; R = reproducibility; U = uncertainty. F = fully reported for the publication's purpose; P = partially reported; N = not reported or not applicable. The coding is descriptive and is not a scientific-quality ranking.

The audit makes the inconsistency visible. Sensor context was fully reported in 24 of 25 sources, but full reporting fell to 12 sources for spectral design, 3 for reproducibility, and 7 for uncertainty. Interferometric processing, ionospheric estimation, and validation were usually addressed, yet the information needed to reproduce parameter choices or attach confidence to the corrected phase was commonly partial. These results support the need for the minimum reporting standard rather than treating incomplete reporting as a purely narrative concern.

5.4. Cross-Sensor Benchmarking

Shared benchmark datasets would allow researchers to process the same observations using different sub-band configurations, filters, and correction approaches. A useful benchmark should represent distinct regimes:

- an L-band scene with strong spatial ionospheric structure;
- a C-band scene with a subtle long-wavelength ionospheric signal;
- an equatorial case with high ionospheric variability;

- a polar or high-latitude case;
- a low-coherence scene;
- a scene containing independently measured deformation; and
- TOPS, Stripmap, and ScanSAR acquisition modes.

Common datasets and metrics would reveal where parameter settings are transferable, where methods become unstable, and which validation measures are most informative. They would also distinguish improvements caused by the estimator from those caused by tuning, filtering, or favorable data conditions. The diversity of published polar, equatorial, C-band, L-band, TOPS, ScanSAR, and large-gradient applications demonstrates both the feasibility and the present lack of a unified benchmark. [2,3,6,8,9,15,18-20,23-25]

Published applications provide complementary real-world evidence but not yet a common benchmark. They include ALOS-based polar ice-velocity validation [3], C-band Sentinel-1 TOPS time-series correction [4], L-band time-series comparisons against independent Global Navigation Satellite System observations [16], equatorial slow-deformation testing [8], and ALOS-2 ScanSAR experiments over the rugged and vegetated Nepal Himalaya [25]. These cases confirm operational relevance across contrasting regimes, but their different bandwidths, coherence thresholds, smoothing scales, validation references, and reported metrics prevent direct quantitative ranking.

5.5. Synthetic Demonstration of the Proposed Reliability Framework

A synthetic 200 × 200-pixel scene representing a 4 × 4 km area was constructed to demonstrate the proposed reporting, validation, and reliability framework. The illustrative L-band observation contained a localized line-of-sight subsidence signal, a spatially smooth ionospheric phase screen, variable coherence, and two imposed low-coherence regions. The numerical outputs are demonstrative and do not represent the measured performance of any satellite mission.

The workflow generated the three linked products recommended in this review: an estimated ionospheric phase screen, a corrected deformation-related phase product, and a spatial reliability classification. Reliability was evaluated from sub-band coherence, valid-pixel support, effective frequency separation, sensitivity to parameter perturbation, and residual phase consistency. The six outputs are shown in **Figure 1**. The synthetic scene, derived numerical outputs, and visualizations presented in Figures 1 and 2 were generated through a common scripted workflow using the stated deformation, ionospheric-phase, coherence, noise, parameter-perturbation, and reliability-classification components. The corresponding synthetic arrays, parameter settings, and figure-generating code are available as described in the Data and Code Availability statement.

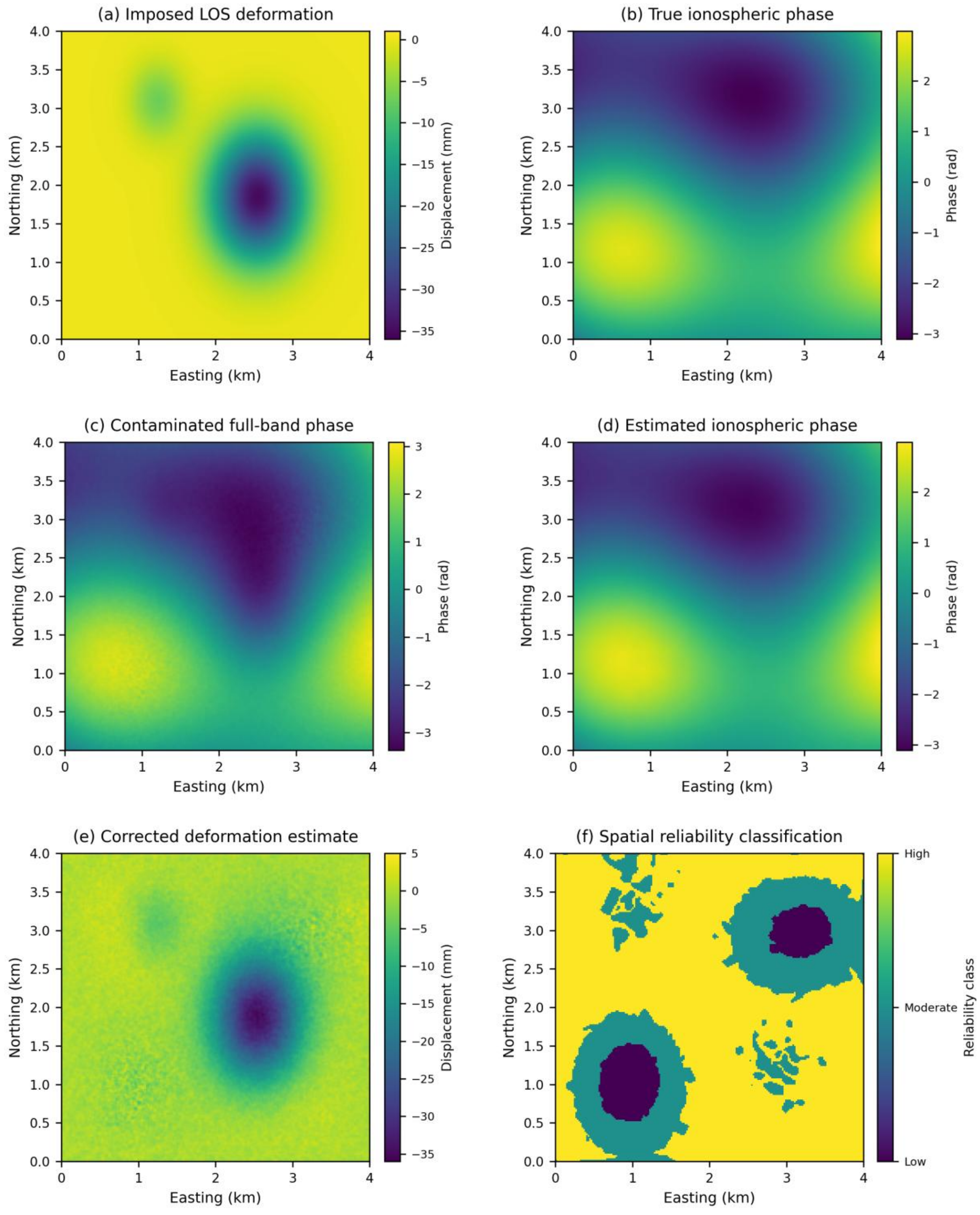

Fig. 1. Synthetic demonstration of the proposed split-spectrum reliability framework: (a) imposed line-of-sight deformation, (b) true ionospheric phase, (c) contaminated full-band phase, (d) estimated ionospheric phase, (e) corrected deformation estimate, and (f) spatial reliability classification.

Three illustrative configurations were then compared. The conservative configuration emphasized high-coherence pixels, the balanced configuration represented a sensitivity-stability compromise, and the aggressive configuration prioritized spatial coverage through wider center-frequency separation and a permissive coherence threshold. Their quantitative comparison is shown in **Figure 2**.

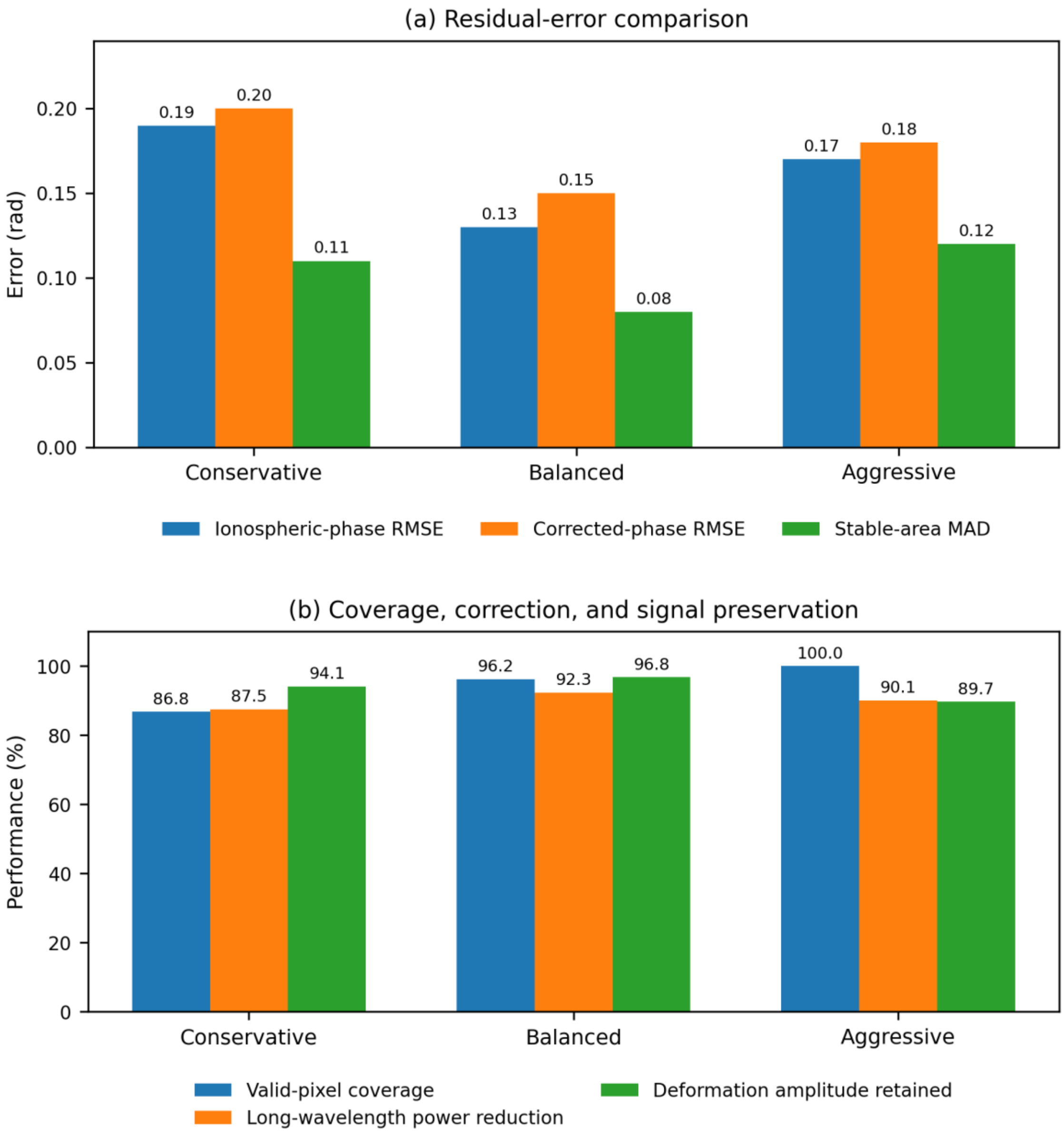

Fig. 2. Illustrative cross-configuration benchmark: (a) ionospheric-phase root-mean-square error, corrected-phase root-mean-square error, and stable-area median absolute deviation; and (b) valid-pixel coverage, long-wavelength phase-power reduction, and preservation of the imposed deformation amplitude.

The numeric comparison is reported here so that Figure 2 remains interpretable at print scale. For the conservative, balanced, and aggressive configurations, respectively, ionospheric-phase root-mean-square error was 0.19, 0.13, and 0.17 rad; corrected-phase root-mean-square error was 0.20, 0.15, and 0.18 rad; and stable-area median absolute deviation was 0.11, 0.08, and 0.12 rad. Valid-pixel coverage was 86.8%, 96.2%, and 100.0%; long-wavelength phase-power reduction was 87.5%, 92.3%, and 90.1%; and preservation of the imposed deformation amplitude was 94.1%, 96.8%, and 89.7%. The balanced configuration therefore produced the lowest illustrative error values while retaining 96.8% of the imposed deformation amplitude and 96.2% valid-pixel coverage. In its reliability product, 66.4% of pixels were classified as high reliability, 26.8% as moderate reliability, and 6.8% as low reliability. These values show how a visually improved interferogram may still differ from alternative configurations in uncertainty, spatial completeness, and signal preservation.

This demonstration is a reproducible reporting template, not an empirical validation of sensor performance. Because the synthetic generator prescribes the deformation, ionospheric phase, noise, and reliability rules, it cannot reproduce all dependencies present in measured data. In particular, it does not test orbit and topographic residuals, spatially variable coregistration errors, burst-edge effects, non-Gaussian decorrelation, phase-unwrapping pathologies, or calibration uncertainty. A mission-level benchmark should therefore replace the known components with independent Global Navigation Satellite System observations, Total Electron Content products, interferometric closure, stable-area statistics, simulated signal-injection tests, or other mission-appropriate evidence. [3,4,8,16,19,25]

6. Operational Significance

The expanding availability of long-wavelength Synthetic Aperture Radar observations makes ionospheric correction increasingly important. NISAR is now in science operations, while the Copernicus ROSE-L mission remains under development; together they illustrate the transition toward sustained L-band observation with wide-swath, repeat-pass capability [27,28]. More frequent acquisitions will improve deformation monitoring, but they will also generate much larger interferometric archives requiring consistent and automated quality assessment. The operational use of NISAR and the forthcoming ROSE-L data stream make transparent performance reporting especially timely [7-9,16,21,23-25,27,28].

Operational systems cannot depend only on visual inspection or manually selected parameters. They need diagnostics indicating whether the split-spectrum estimate is sufficiently supported by the available bandwidth, coherence, and frequency separation. The practical question is no longer only whether the ionosphere was corrected, but how uncertain the correction is, how it was validated, and whether it can be reproduced.

7. Conclusion

Split-spectrum interferometry is one of the most physically grounded approaches for separating dispersive ionospheric effects from non-dispersive InSAR phase. The reporting audit shows that sensor context is usually clear, whereas complete spectral-design, reproducibility, and uncertainty information remains uncommon. Methodological maturity should therefore not be judged only by the number of correction algorithms. Transparent parameter reporting, covariance-aware uncertainty propagation, independent validation, and reproducibility across sensors and environments are equally necessary. The strongest opportunity for the InSAR community is a shared standard through which present and future methods can be compared. A corrected interferogram should be accompanied not only by a cleaner phase pattern, but also by evidence explaining why that pattern can be trusted.

Conflicts of Interest

The author declares that there is no conflict of interest regarding the publication of this paper.

Funding Statement

The author received no financial support for the publication of this article.

Author Contribution Statement

MS conceived the review, selected and interpreted the literature, conducted the reporting-coverage audit, developed the reporting and reliability framework, prepared the synthetic demonstration, and wrote and approved the manuscript.

Data and Code Availability

No external observational dataset was used in the synthetic demonstration. The synthetic input arrays, derived numerical outputs, parameter settings, and figure-generating code underlying Figures 1 and 2 are available from the corresponding author upon reasonable request.

AI-Assisted Tools Statement

Generative AI-assisted tools were used to support language refinement, structural editing, bibliographic organization, and development and debugging of Python code for the synthetic demonstration. The author independently reviewed and verified the scientific arguments, equations, source-selection decisions, numerical outputs, references, interpretations, and conclusions, and assumes full responsibility for the accuracy, originality, and integrity of the preprint.

References

[1] G. Gomba, A. Parizzi, F. De Zan, M. Eineder, and R. Bamler, "Toward Operational Compensation of Ionospheric Effects in SAR Interferograms: The Split-Spectrum Method," IEEE Transactions on Geoscience and Remote Sensing, vol. 54, no. 3, pp. 1446–1461, 2016. doi: 10.1109/TGRS.2015.2481079.

[2] G. Gomba, F. Rodríguez González, and F. De Zan, "Ionospheric Phase Screen Compensation for the Sentinel-1 TOPS and ALOS-2 ScanSAR Modes," IEEE Transactions on Geoscience and Remote Sensing, vol. 55, no. 1, pp. 223–235, 2017. doi: 10.1109/TGRS.2016.2604461.

[3] H. Liao, F. J. Meyer, B. Scheuchl, J. Mouginot, I. Joughin, and E. Rignot, "Ionospheric Correction of InSAR Data for Accurate Ice Velocity Measurement at Polar Regions," Remote Sensing of Environment, vol. 209, pp. 166–180, 2018. doi: 10.1016/j.rse.2018.02.048.

[4] C. Liang, P. Agram, M. Simons, and E. J. Fielding, "Ionospheric Correction of InSAR Time Series Analysis of C-Band Sentinel-1 TOPS Data," IEEE Transactions on Geoscience and Remote Sensing, vol. 57, no. 9, pp. 6755–6773, 2019. doi: 10.1109/TGRS.2019.2908494.

[5] F. Dou, X. Lv, Q. Chen, et al., "The Impact of SAR Parameter Errors on the Ionospheric Correction Based on the Range-Doppler Model and the Split-Spectrum Method," Remote Sensing, vol. 12, no. 10, Art. no. 1607, 2020. doi: 10.3390/rs12101607.

[6] B. Zhang, W. Zhu, X. Ding, et al., "A Review of Methods for Mitigating Ionospheric Artifacts in Differential SAR Interferometry," Geodesy and Geodynamics, vol. 13, no. 2, pp. 160–169, 2022. doi: 10.1016/j.geog.2021.12.001.

[7] W. Mao, X. Wang, G. Liu, S. Pirasteh, R. Zhang, H. Lin, Y. Xie, W. Xiang, Z. Ma, and P. Ma, "Time Series InSAR Ionospheric Delay Estimation, Correction, and Ground Deformation Monitoring with Reformulating Range Split-Spectrum Interferometry," IEEE Transactions on Geoscience and Remote Sensing, vol. 61, Art. no. 5213118, 2023. doi: 10.1109/TGRS.2023.3298919.

[8] L. Marconato, M.-P. Doin, L. Audin, and E. Pathier, "Ionospheric Compensation in L-Band InSAR Time-Series: Performance Evaluation for Slow Deformation Contexts in Equatorial Regions," Science of Remote Sensing, vol. 9, Art. no. 100113, 2024. doi: 10.1016/j.srs.2023.100113.

[9] X. Wang, W. Mao, R. Zhang, and G. Liu, "Synthetic Aperture Radar Split-Spectrum Interferometry: Principles, Applications, and Prospects," National Remote Sensing Bulletin, vol. 30, no. 4, pp. 777–797, 2026. doi: 10.11834/jrs.20265230.

[10] K. E. Mattar and A. L. Gray, "Reducing Ionospheric Electron Density Errors in Satellite Radar Interferometry Applications," Canadian Journal of Remote Sensing, vol. 28, no. 4, pp. 593–600, 2002. doi: 10.5589/m02-051.

[11] F. Meyer, R. Bamler, N. Jakowski, and T. Fritz, "The Potential of Low-Frequency SAR Systems for Mapping Ionospheric TEC Distributions," IEEE Geoscience and Remote Sensing Letters, vol. 3, no. 4, pp. 560–564, 2006. doi: 10.1109/LGRS.2006.882148.

[12] U. Wegmüller, C. Werner, T. Strozzi, and A. Wiesmann, "Ionospheric Electron Concentration Effects on SAR and InSAR," in Proceedings of the IEEE International Geoscience and Remote Sensing Symposium, pp. 3731–3734, 2006. doi: 10.1109/IGARSS.2006.956.

[13] F. J. Meyer and J. B. Nicoll, "The Impact of the Ionosphere on Interferometric SAR Processing," in Proceedings of the IEEE International Geoscience and Remote Sensing Symposium, vol. 2, pp. II-391–II-394, 2008. doi: 10.1109/IGARSS.2008.4779010.

[14] R. Brcic, A. Parizzi, M. Eineder, R. Bamler, and F. Meyer, "Estimation and Compensation of Ionospheric Delay for SAR Interferometry," in Proceedings of the 2010 IEEE International Geoscience and Remote Sensing Symposium, Honolulu, HI, USA, pp. 2908–2911, 2010. doi: 10.1109/IGARSS.2010.5652231.

[15] H.-S. Jung, D.-T. Lee, Z. Lu, and J.-S. Won, "Ionospheric Correction of SAR Interferograms by Multiple-Aperture Interferometry," IEEE Transactions on Geoscience and Remote Sensing, vol. 51, no. 5, pp. 3191–3199, 2013. doi: 10.1109/TGRS.2012.2218660.

[16] H. Fattahi, M. Simons, and P. Agram, "InSAR Time-Series Estimation of the Ionospheric Phase Delay: An Extension of the Split Range-Spectrum Technique," IEEE Transactions on Geoscience and Remote Sensing, vol. 55, no. 10, pp. 5984–5996, 2017. doi: 10.1109/TGRS.2017.2718566.

[17] U. Wegmüller, C. Werner, O. Frey, C. Magnard, and T. Strozzi, "Reformulating the Split-Spectrum Method to Facilitate the Estimation and Compensation of the Ionospheric Phase in SAR Interferograms," Procedia Computer Science, vol. 138, pp. 318–325, 2018. doi: 10.1016/j.procs.2018.10.045.

[18] H. Luo, Z. Li, J. Chen, C. Pearson, M. Wang, W. Lv, and H. Ding, "Integration of Range Split Spectrum Interferometry and Conventional InSAR to Monitor Large Gradient Surface Displacements," International Journal of Applied Earth Observation and Geoinformation, vol. 74, pp. 130–137, 2019. doi: 10.1016/j.jag.2018.09.004.

[19] W.-T. Liao, K.-H. Tseng, I.-T. Lee, A. Liibusk, J.-C. Lee, J.-Y. Liu, C.-P. Chang, and Y.-C. Lin, "Sentinel-1 Interferometry with Ionospheric Correction from Global and Local TEC Maps for Land Displacement Detection in Taiwan," Advances in Space Research, vol. 65, no. 5, pp. 1447–1465, 2020. doi: 10.1016/j.asr.2019.11.041.

[20] W. Mao, X. Wang, G. Liu, R. Zhang, Y. Shi, and S. Pirasteh, "Estimation and Compensation of Ionospheric Phase Delay for Multi-Aperture InSAR: An Azimuth Split-Spectrum Interferometry Approach," IEEE Transactions on Geoscience and Remote Sensing, vol. 60, Art. no. 5209414, 2022. doi: 10.1109/TGRS.2021.3095272.

[21] Y.-Y. Wu and A. Madson, "Error Sources of Interferometric Synthetic Aperture Radar Satellites," Remote Sensing, vol. 16, no. 2, Art. no. 354, 2024. doi: 10.3390/rs16020354.

[22] G. Li, Z. Hu, Y. Wang, Z. Dong, and H. Li, "Correction of Ionospheric Phase in SAR Interferometry Considering Wavenumber Shift," Remote Sensing, vol. 16, no. 14, Art. no. 2555, 2024. doi: 10.3390/rs16142555.

[23] U. Wegmüller, C. Werner, O. Frey, and C. Magnard, "Estimation and Compensation of the Ionospheric Path Delay Phase in PALSAR-3 and NISAR-L Interferograms," Atmosphere, vol. 15, no. 6, Art. no. 632, 2024. doi: 10.3390/atmos15060632.

[24] Y. Ji, Z. Dong, Y. Zhang, C. Wang, C. Hu, and Z. Xu, "Transionospheric Synthetic Aperture Radar Observation: A Comprehensive Review," IEEE Geoscience and Remote Sensing Magazine, vol. 13, no. 2, pp. 273–313, 2025. doi: 10.1109/MGRS.2024.3454635.

[25] S. Nagaoka, Y. Takada, and Y. Morishita, "Improved Application of the Split-Spectrum Method to L-Band Interferograms for Ionospheric Phase Mitigation: A Practical Recipe," Earth, Planets and Space, vol. 77, Art. no. 82, 2025. doi: 10.1186/s40623-025-02206-9.

[26] European Space Agency, "Ionospheric Correction Operator," SNAP Online Help, version 13.0.0. [Online]. Available: https://step.esa.int/main/wp-content/help/versions/13.0.0/snap-toolboxes/eu.esa.microwavetbx.sar.op.insar.ui/operators/IonosphericCorrectionOp.html [Accessed: Aug. 5, 2026].

[27] National Aeronautics and Space Administration, "Mission Overview—NISAR Quick Facts," NASA Science, updated June 2, 2026. [Online]. Available: https://science.nasa.gov/mission/nisar/mission-overview/ [Accessed: Aug. 5, 2026].

[28] European Space Agency, "ROSE-L Radar Unfolds in Crucial Ground Test," Apr. 8, 2026. [Online]. Available: https://www.esa.int/Applications/Observing_the_Earth/Copernicus/ROSE-L_radar_unfolds_in_crucial_ground_test [Accessed: Aug. 5, 2026].